

G. Pavia, M. A. Passmore

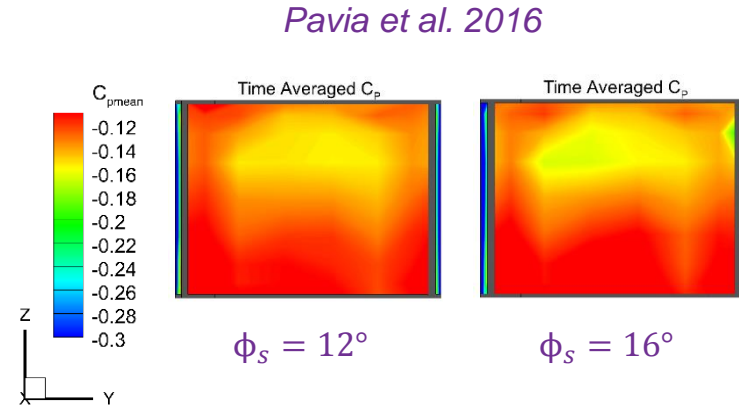
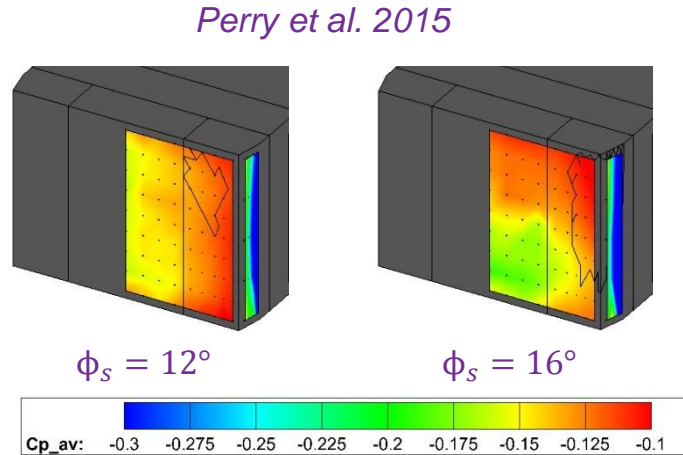
# **CHARACTERISATION OF THE LOW-FREQUENCY WAKE DYNAMICS FOR A SQUARE-BACK VEHICLE EQUIPPED WITH SIDE TRAILING EDGE TAPERS**

# Background

- The turbulent wake past square-back bodies shows a strong bimodal behaviour, whose characteristic time  $T_l \approx 10^3 W/U_\infty$  is about 2 or 3 orders of magnitude larger than the natural time for vortex shedding (*Grandemange et al., 2013b*).
- For a square-back model with  $W > H$  the wake has been observed to switch between two lateral symmetry breaking states. (*Grandemange et al., 2013a*).
- An upwash or downwash dominated, lateral symmetry preserving state can be seen during the switch between bi-stable states. (*Pavia et al., 2018*).
- The bi-stable mode is seen to weaken as the distance between the top and bottom shear layers is reduced, for example by applying small tapers to the model horizontal trailing edges (*Perry et al., 2016b*).
- The application of similar tapers to the model's side edges is able to 'lock' the wake in a vertically asymmetric, stable state (*Pavia et al., 2016*).

# Background

In these conditions, a  $\approx 13\%$  improvement over the square-back case has been reported in the pressure recovery over the model rear facing surfaces (*Perry et al. 2015, Pavia et al. 2016*)



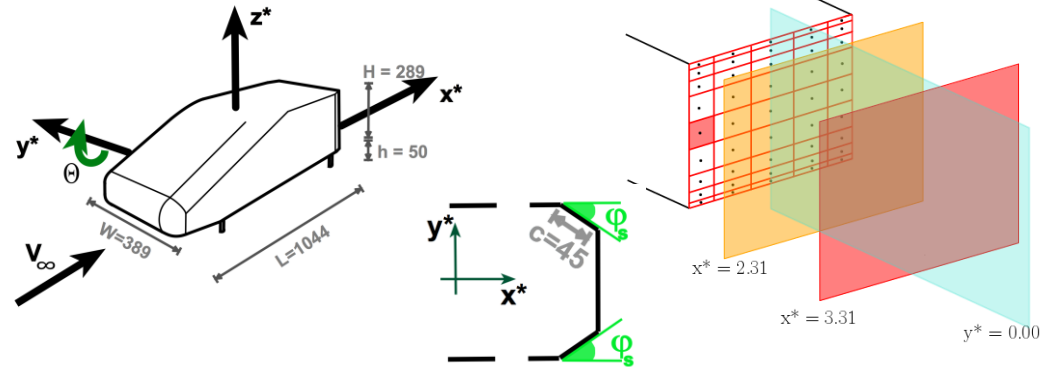
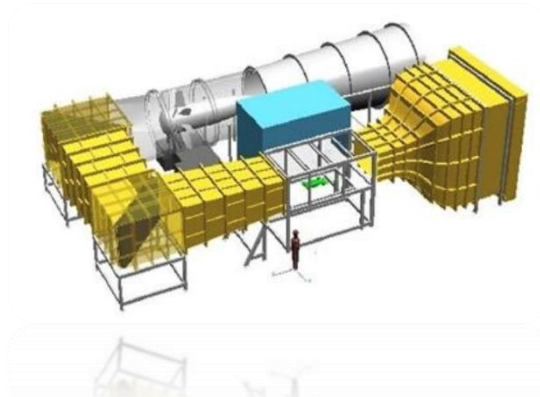
Different wake orientations, however, are reported in the literature.

# Aim of the Study

1. Identify the changes in the wake topology responsible for the drag reduction.
2. Characterise the transition from a laterally asymmetric, bi-stable wake to a vertically asymmetric, stable wake.
3. Isolate the cause of the different wake orientations reported in the literature.

# Experimental Methodology

An experimental campaign was carried out in the Loughborough University Large Wind Tunnel using the Windsor body.



Small tapers (with chamfer angles  $\varphi$  equal to  $6^\circ$ ,  $12^\circ$ ,  $16^\circ$  and  $20^\circ$ ) were applied to the model vertical trailing edges.

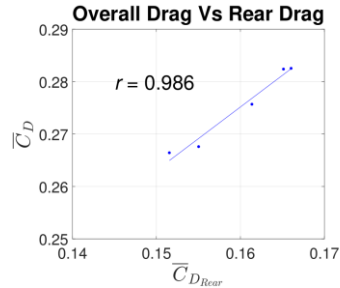
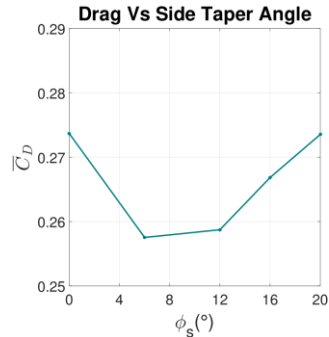
All tests were performed at a tunnel free stream velocity of 40 m/s, resulting in a Reynolds number  $Re_H$  of  $7.7 \cdot 10^5$ .

Balance measurements, pressure tappings and PIV acquisitions were performed.

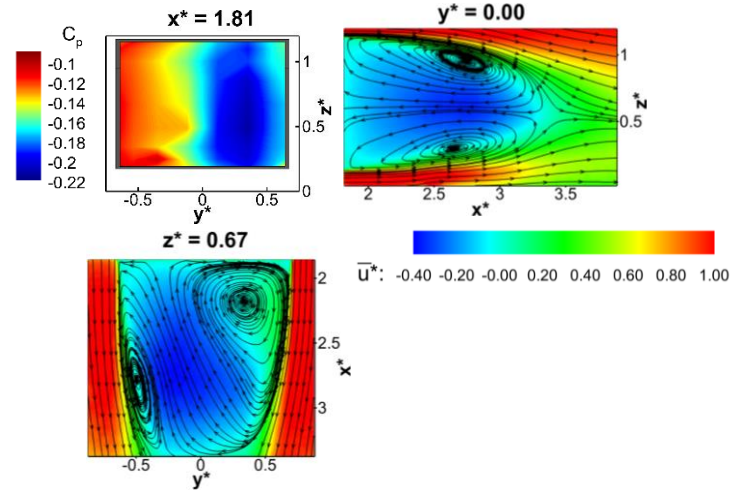
The sensitivity of the flow field to variations of the model pitch angle was also assessed.

1. Identify the changes in the wake topology responsible for the drag reduction.

## Time Averaged Results



$\phi_s = 0^\circ$ , R State  
(Perry et al., 2016b)



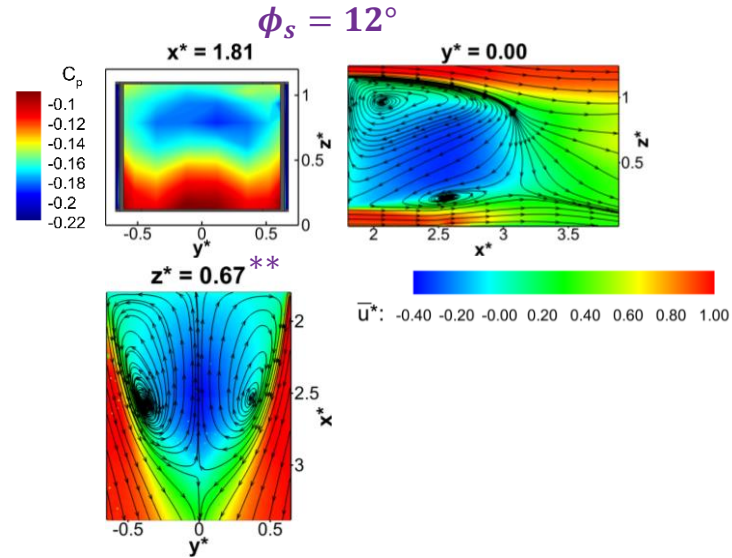
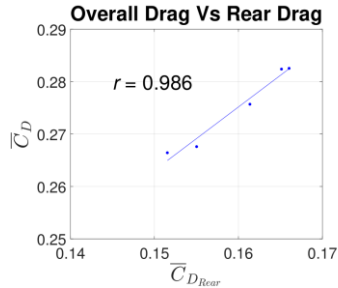
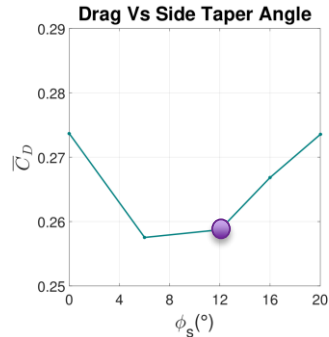
A  $\approx 6\%$  drag reduction over the square-back case is seen for  $6^\circ \leq \phi_s \leq 12^\circ$ , in agreement with the findings of Perry et al. 2015.

The drag reduction is driven by changes in the pressure distribution over the model rear facing surfaces.

The improved pressure recovery over the model base is to be ascribed to changes in the wake topology.

1. Identify the changes in the wake topology responsible for the drag reduction.

# Time Averaged Results

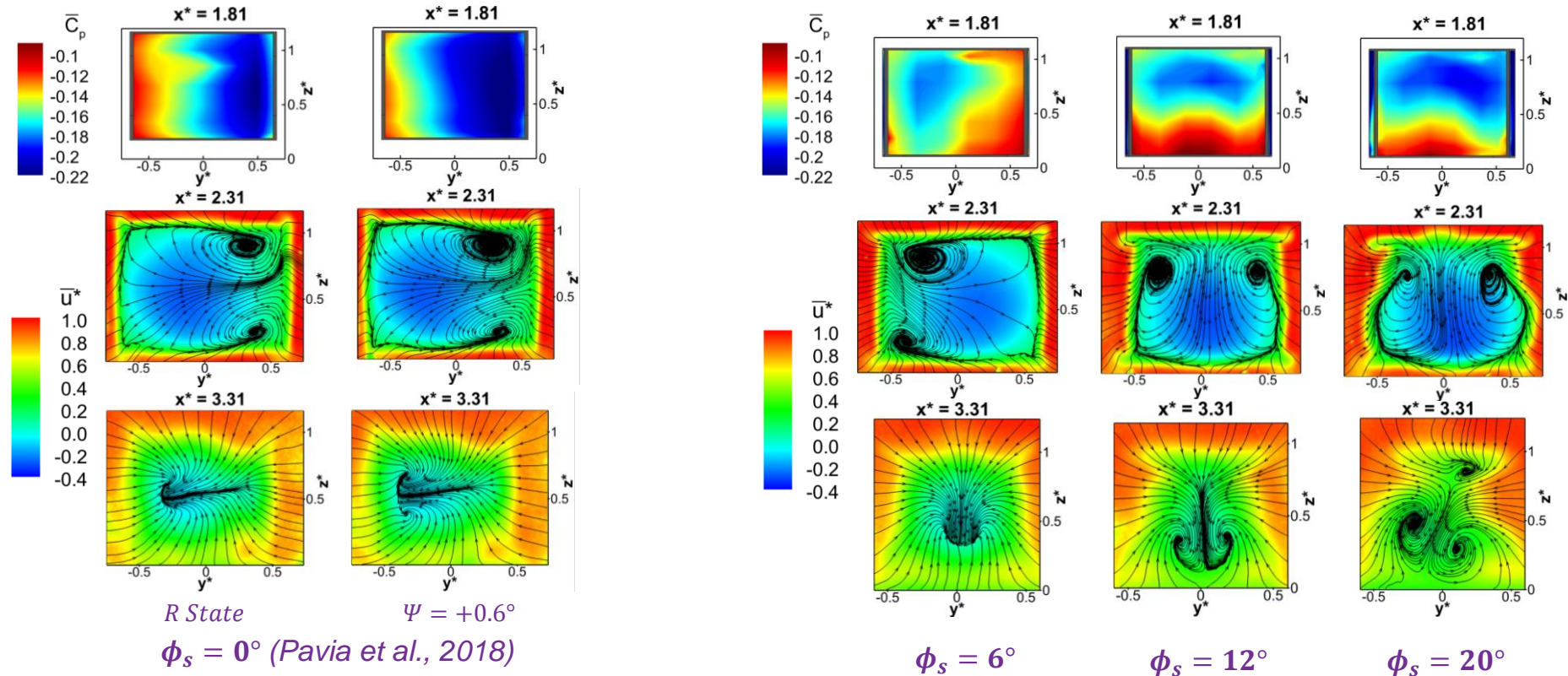


$\Delta \bar{C}_D$	$\Delta \bar{C}_{D_{Rear}}$	$\Delta \bar{C}_{D_{Base}}$
5.5%	6.6%	15.1%

The circular vortex responsible for the suction zone seen in each lateral symmetry breaking state (for the square-back case) is moved towards the top trailing edge and 'stretched' in the streamwise direction.

2. Characterise the transition from a laterally asymmetric, bi-stable wake to a vertically asymmetric, stable wake.

# Wake Topology

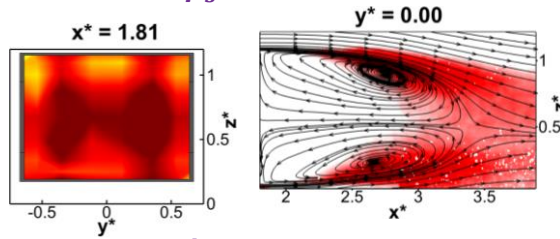




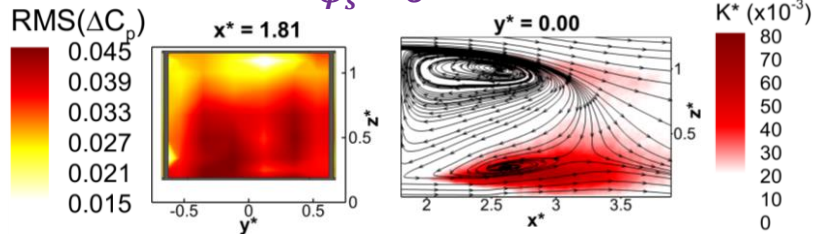
2. Characterise the transition from a laterally asymmetric, bi-stable wake to a vertically asymmetric, stable wake.

# Unsteady Results

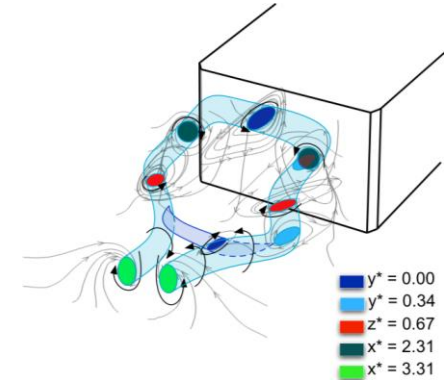
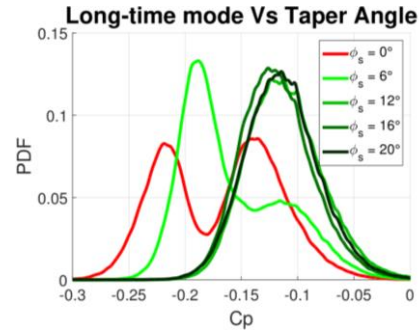
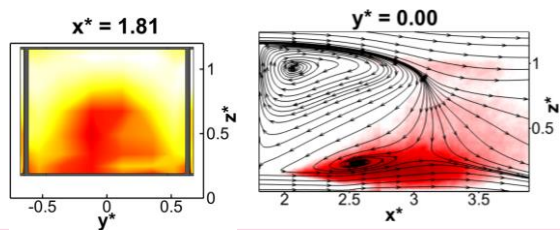
$\phi_s = 0^\circ$



$\phi_s = 6^\circ$



$\phi_s = 12^\circ$



The level of unsteadiness in the pressure datasets is reduced as  $\phi_s$  increases.

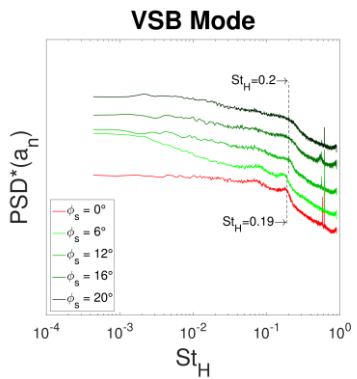
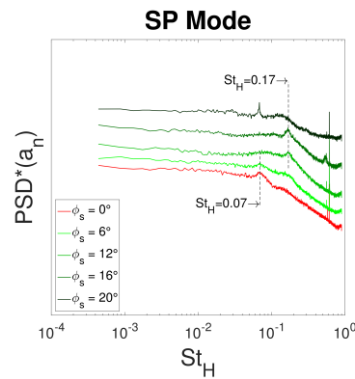
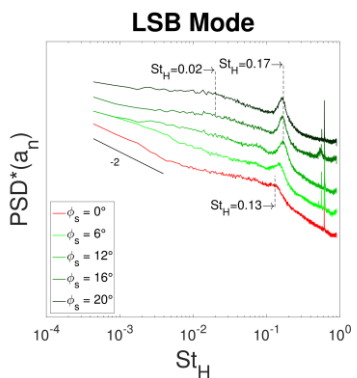
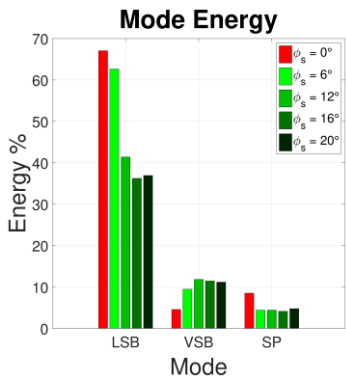
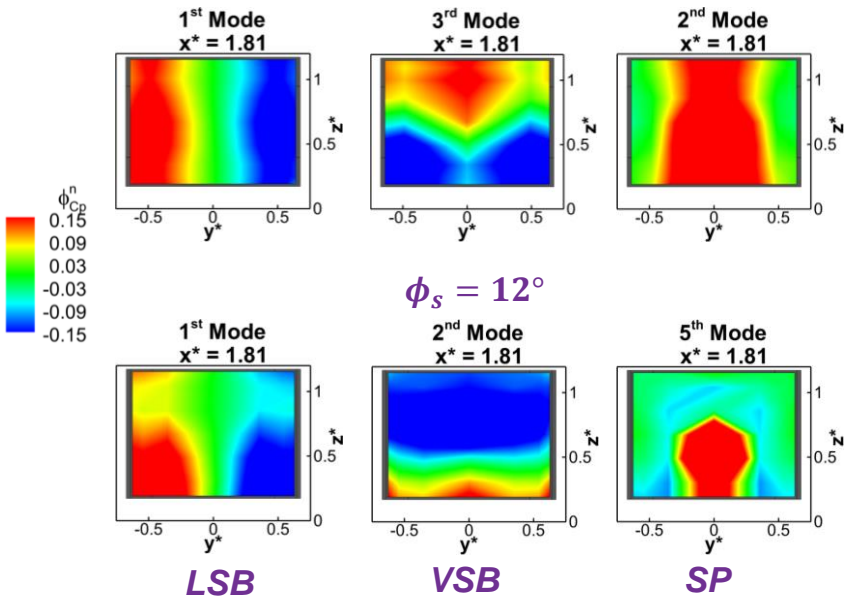
The upper recirculation becomes more stable.

The wake locks in a vertical symmetry breaking state.

2. Characterise the transition from a laterally asymmetric, bi-stable wake to a vertically asymmetric, stable wake.

# POD Modes (base pressure)

$\phi_s = 0^\circ$  (Pavia et al., 2018)



The energy content of the LSB mode is noticeably reduced.

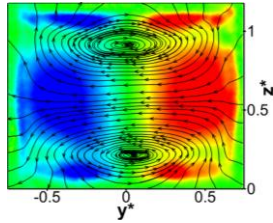
A lateral flapping motion is seen at  $St_H = 0.17$ .

2. Characterise the transition from a laterally asymmetric, bi-stable wake to a vertically asymmetric, stable wake.

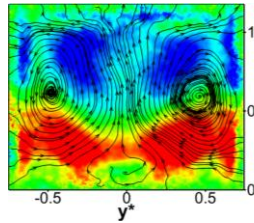
# POD Modes (velocity fields)

$\phi_s = 0^\circ$  (Pavia et al., 2018)

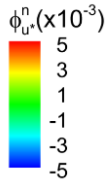
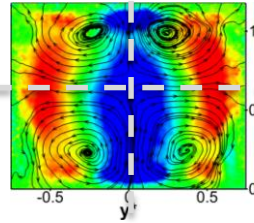
1<sup>st</sup> Mode  
 $x^* = 2.31$



3<sup>rd</sup> Mode  
 $x^* = 2.31$

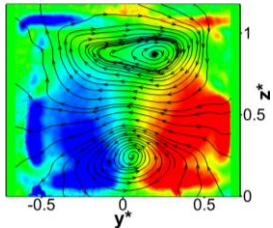


2<sup>nd</sup> Mode  
 $x^* = 2.31$



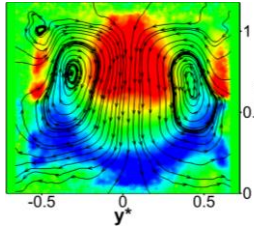
$\phi_s = 12^\circ$

1<sup>st</sup> Mode  
 $x^* = 2.31$



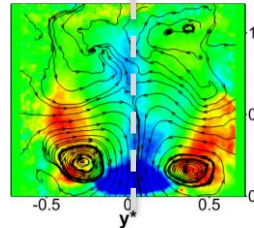
LSB

2<sup>nd</sup> Mode  
 $x^* = 2.31$



VSB

3<sup>rd</sup> Mode  
 $x^* = 2.31$

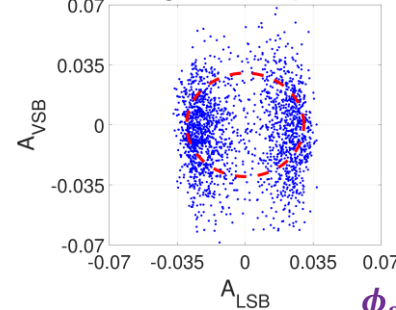


SP

A plane of symmetry is lost in the SP mode.

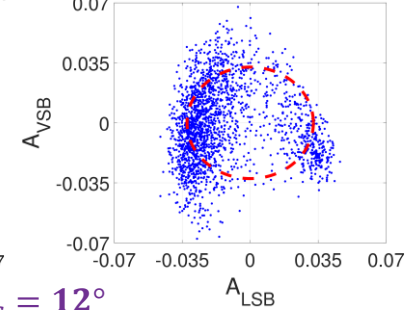
$\phi_s = 0^\circ$

POD Eigenvectors (Unsorted)



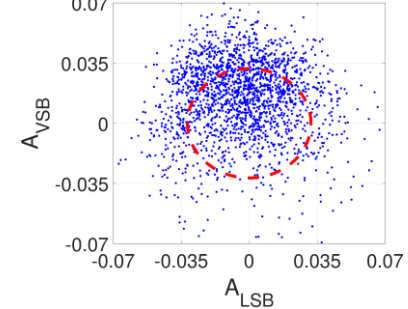
$\phi_s = 6^\circ$

POD Eigenvectors (Unsorted)



$\phi_s = 12^\circ$

POD Eigenvectors (Unsorted)

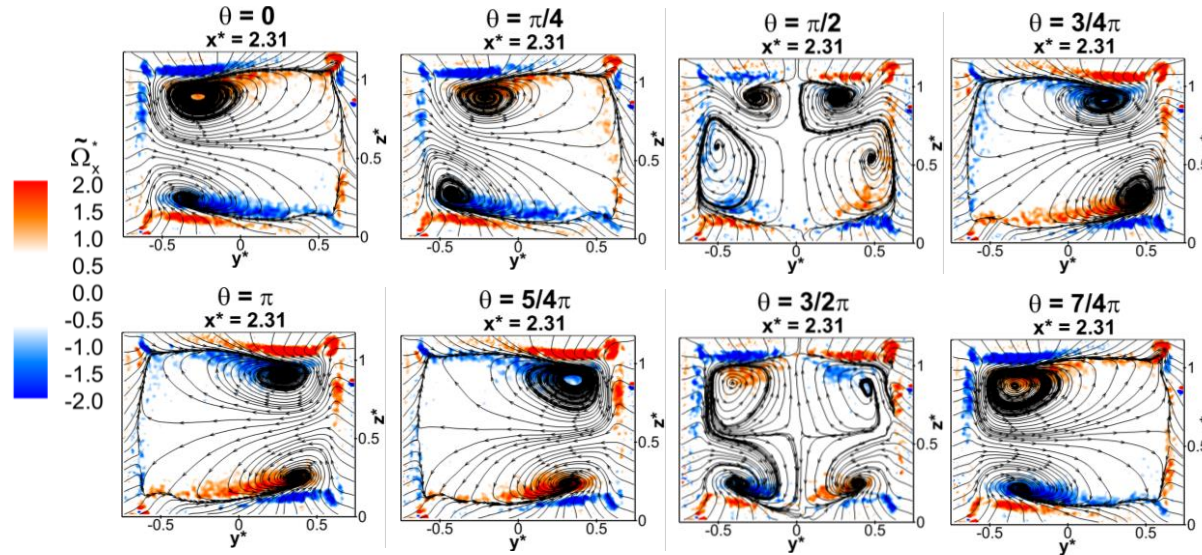


The points in the scatter plot between  $A_{VSB}(t)$  and  $A_{LSB}(t)$  tend to cluster around a new attractor.

2. Characterise the transition from a laterally asymmetric, bi-stable wake to a vertically asymmetric, stable wake.

## POD Filtered Phase Averaged Velocity Field

$\phi_s = 0^\circ$  (Pavia et al., 2018)

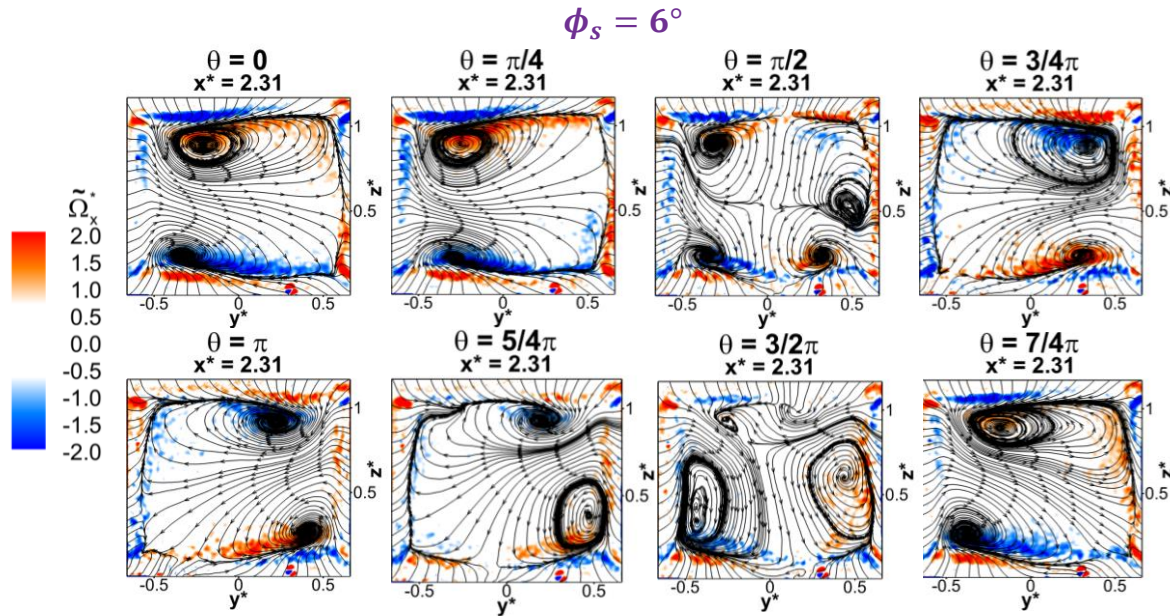


The wake randomly switches between two lateral symmetry breaking states.

During the switch, two different lateral symmetry preserving states can be seen, each characterised by the predominance of either the lower recirculation or the upper recirculation.

2. Characterise the transition from a laterally asymmetric, bi-stable wake to a vertically asymmetric, stable wake.

## POD Filtered Phase Averaged Velocity Field



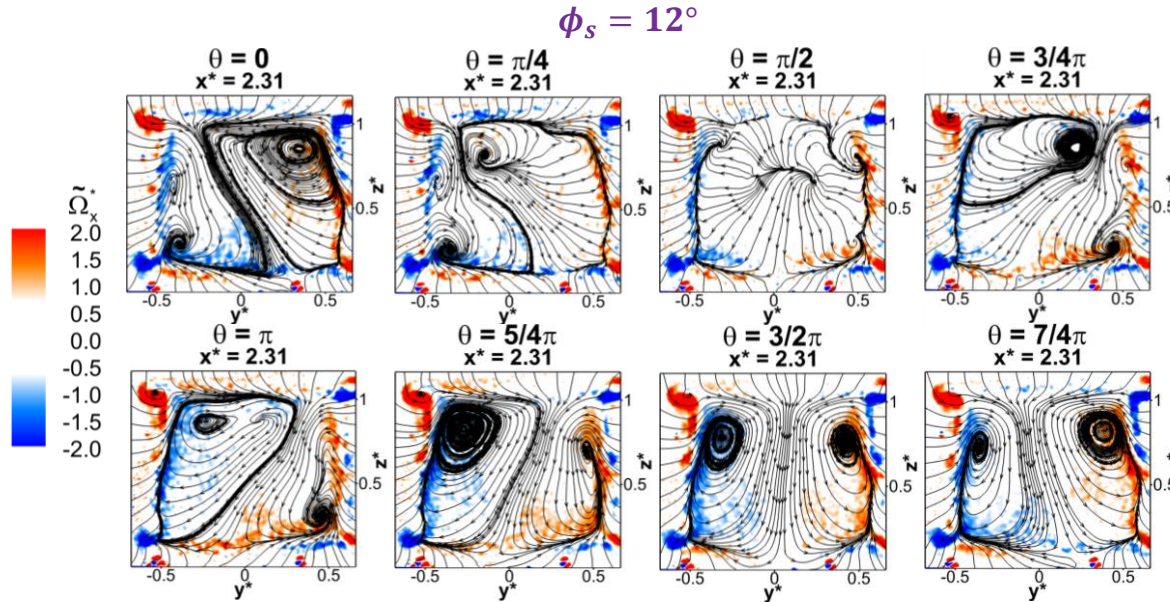
The two lateral symmetry breaking states can still be seen.

The two lateral symmetry preserving states are no longer mirror images of each other.

The downwash dominated state tends to become predominant.

2. Characterise the transition from a laterally asymmetric, bi-stable wake to a vertically asymmetric, stable wake.

## POD Filtered Phase Averaged Velocity Field



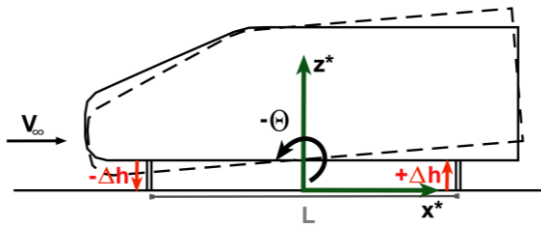
The downwash dominated state is the only stable configuration of the wake.

Every time the wake 'moves' towards a lateral symmetry breaking state, the vortical structures lose coherence.

3. Isolate the cause of the different wake orientations reported in the literature.

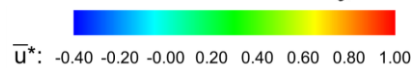
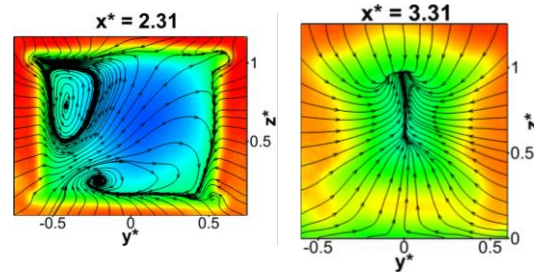
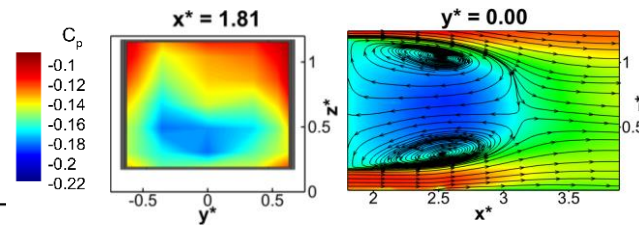
# Pitch Angle Variations

## Wake Topology

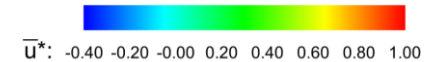
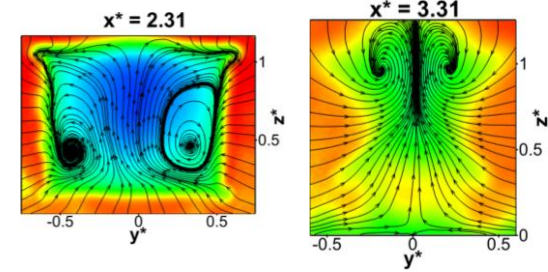
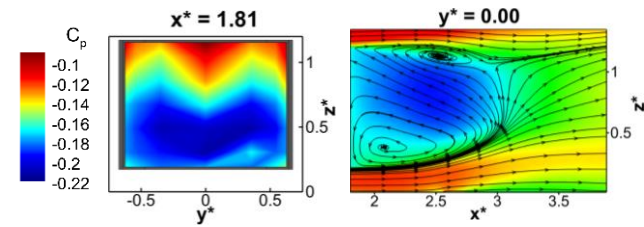


The time averaged wake topology is seen to rotate around the centre of the model base, when the pitch angle  $\theta$  is decreased.

$$\phi_s = 12^\circ, \theta = -1.0^\circ$$



$$\phi_s = 12^\circ, \theta = -2.0^\circ$$



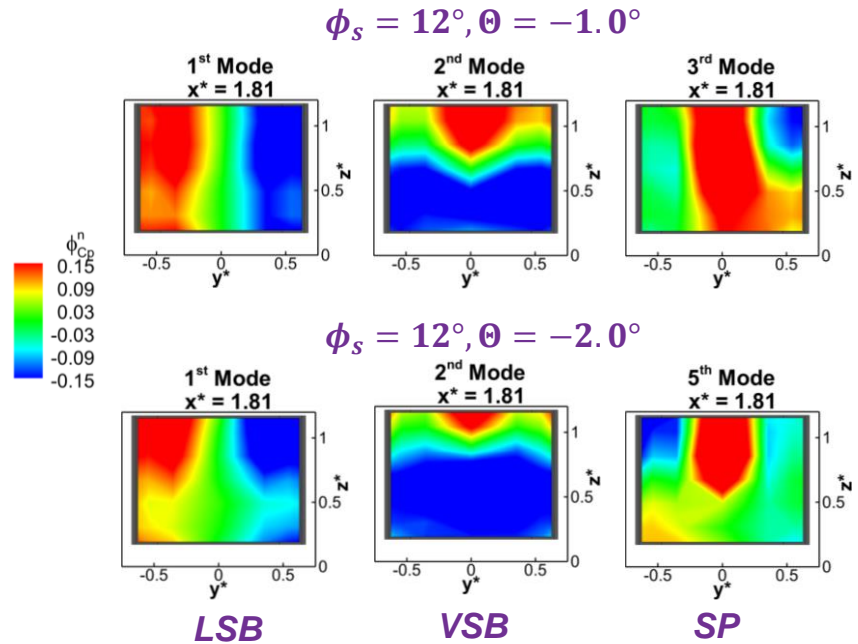
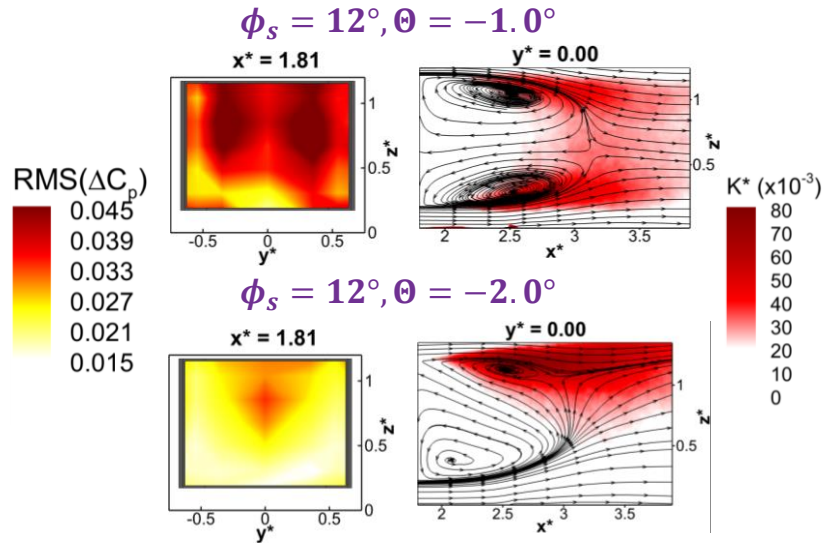
For  $\theta = -1^\circ$ , the wake recovers symmetry in the vertical direction.

In these conditions, a 4.7% reduction in the base drag over the same configuration tested at  $\theta = 0^\circ$  is observed.

3. Isolate the cause of the different wake orientations reported in the literature.

# Pitch Angle Variations

## Unsteady Results



As the symmetry in the vertical direction is recovered, an increase in the level of unsteadiness is seen in both pressure and PIV data.

For  $\Theta = -1^\circ$ , coherent pressure variations are seen over the entire model base

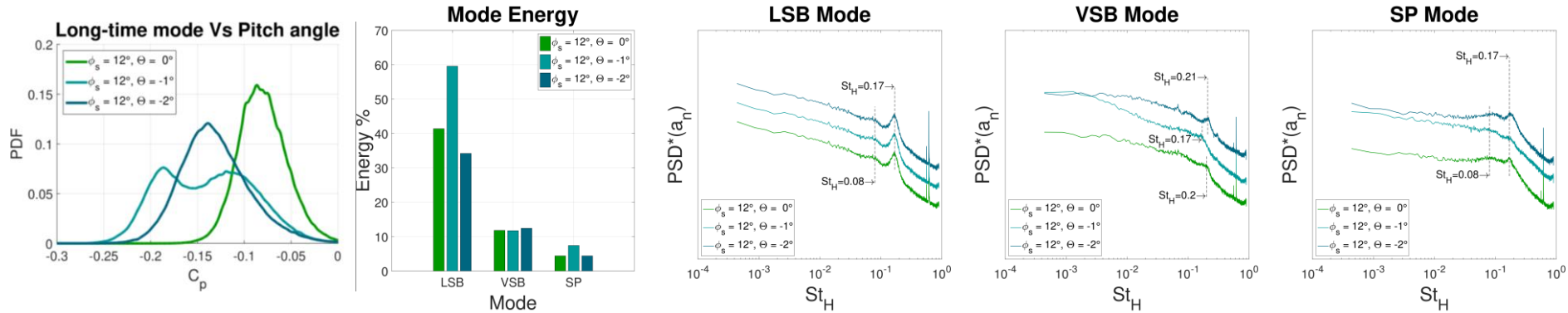


3. Isolate the cause of the different wake orientations reported in the literature.

# Pitch Angle Variations

## Unsteady Results

No significant changes are seen in the global oscillating modes.



The restoration of a multi-stable condition is highlighted by the wider distribution seen in the values of  $C_p$  recorded by one of the taps placed in the region of high pressure fluctuation.

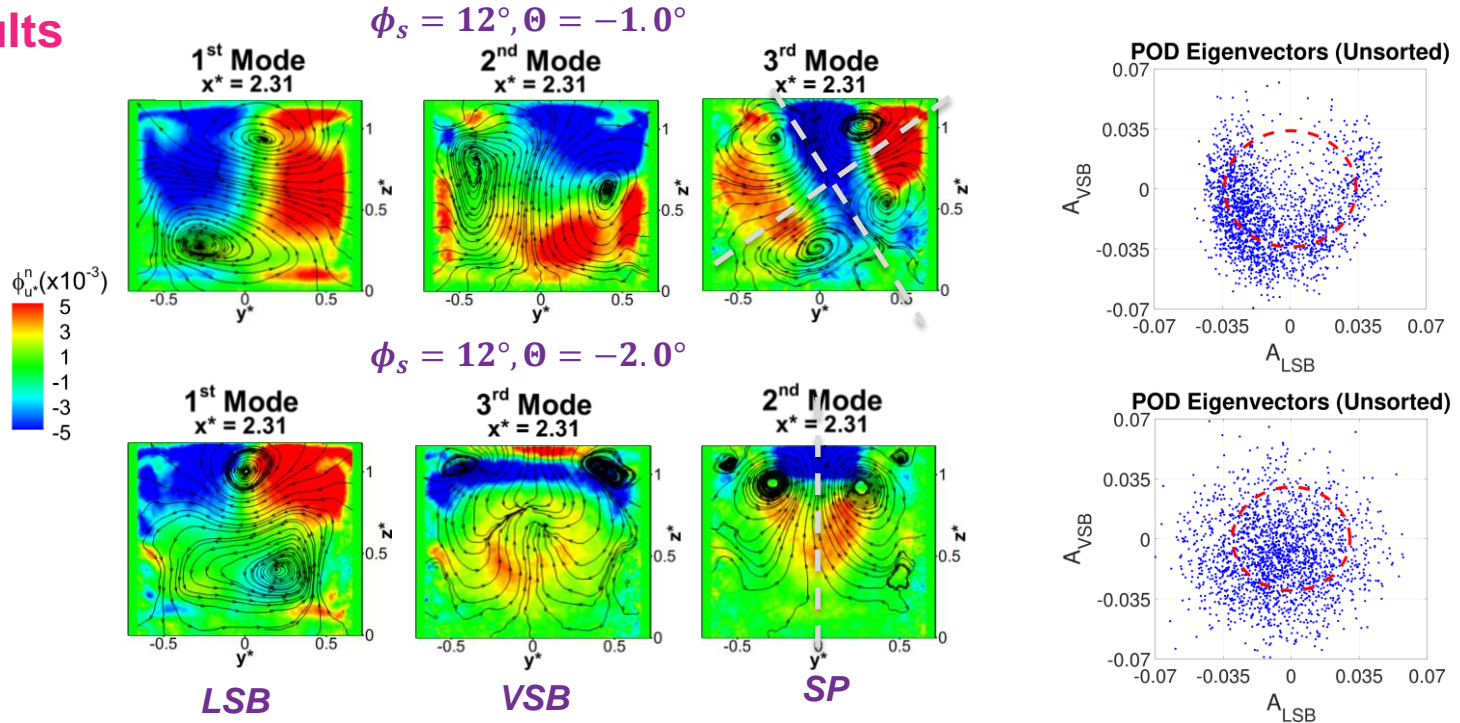
An increase in the energy content of the LSB mode and the SP mode is also observed.

**The lowest drag case is not the most stable case!**

3. Isolate the cause of the different wake orientations reported in the literature.

# Pitch Angle Variations

## Unsteady Results

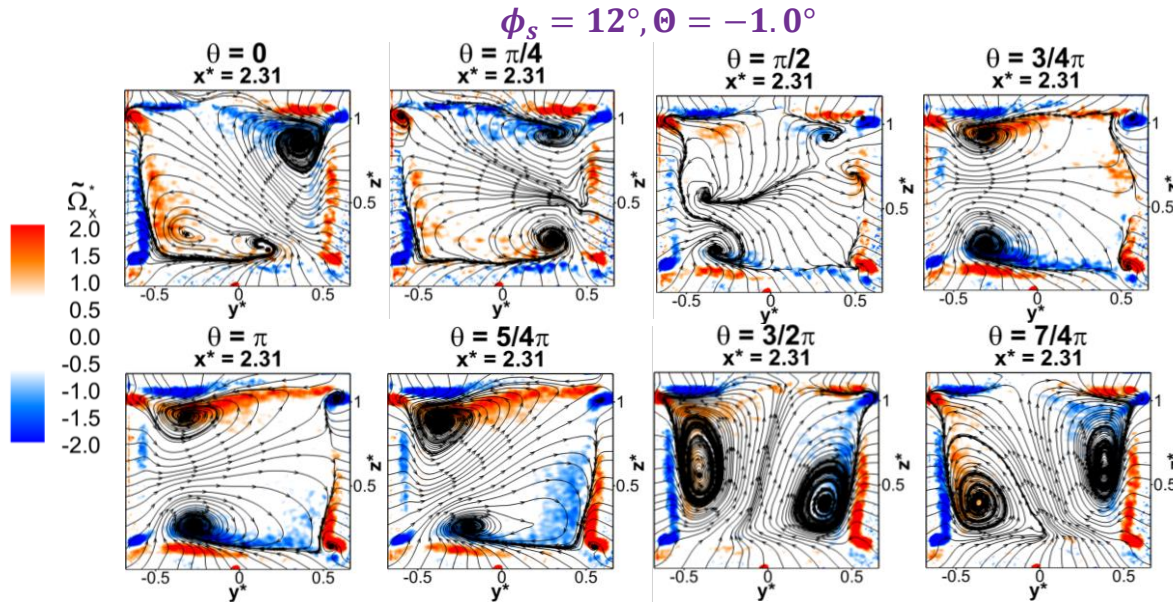


A second plane of symmetry appears in the SP mode.

3. Isolate the cause of the different wake orientations reported in the literature.

# Pitch Angle Variations

## POD Filtered Phase Averaged Velocity Field

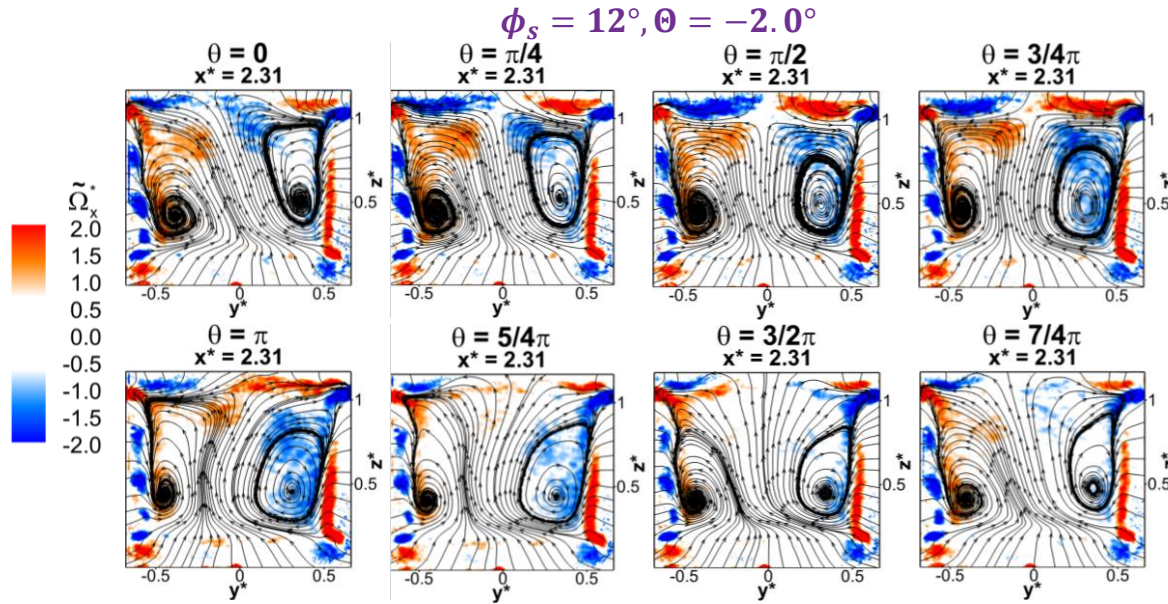


The wake is seen to switch between three different configurations: two lateral symmetry breaking states and a vertical symmetry breaking state.

3. Isolate the cause of the different wake orientations reported in the literature.

# Pitch Angle Variations

## POD Filtered Phase Averaged Velocity Field



The wake locks in an upwash dominated, vertical symmetry breaking state.

# Conclusions

The effects of side trailing edge tapers on the wake past a simplified square-back geometry have been investigated by means of balance measurements, pressure tappings and PIV acquisitions:

- The wake has been seen to switch from a lateral symmetry breaking state to a vertical symmetry breaking state. The drag reduction reported in the literature has been shown to be a consequence of the stretching of the circular vortex responsible for the creation of the suction zone in any of the symmetry breaking states.
- As the chamfer angle is increased, the lateral symmetry breaking mode is weakened. A downwash dominated, vertical symmetry breaking state appears. This state eventually becomes the wake's most stable configuration for  $\phi_s \geq 12^\circ$ .
- The wake orientation in the vertical direction has been shown to be very sensitive to small variations of the model pitch angle  $\Theta$ . This high level of sensitivity may be the cause of the differences in the results reported in the literature.
- The recovery of symmetry in the vertical direction in the time averaged wake has been reported to yield a 4.7% base drag reduction over the same configuration tested at  $\Theta = 0^\circ$ . This, however, has not been found to be linked with the stabilisation of the wake.

# References

- Grandemange, M., Gohlke, M., and Cadot, O. (2013b). *Turbulent wake past a three-dimensional blunt body. Part 1. Global modes and bi-stability*. *Journal of Fluid Mechanics*, 722:51–84.
- Grandemange, M., Gohlke, M., & Cadot, O. (2013). *Bi-stability in the turbulent wake past parallelepiped bodies with various aspect ratios and wall effects*. *Physics of Fluids*, 25(9), 095103.
- Pavia, G., Passmore, M., & Gaylard, A. P. (2016). *Influence of short rear end tapers on the unsteady base pressure of a simplified ground vehicle*. *SAE Technical Paper 2016-01-1590*, 2016, doi:10.4271/2016-01-1590.
- Pavia, G., Passmore, M., & Sardu, C. (2018). *Evolution of the bi-stable wake of a square-back automotive shape*. *Experiments in Fluids*, 59(1), 20.
- Perry, A. K., Passmore, M., & Finney, A. (2015). *Influence of Short Rear End tapers on the Base Pressure of a Simplified Vehicle*. *SAE International Journal of Passenger Cars-Mechanical Systems*, 8(2015-01-1560), 317-327.
- Perry, A.-K., Pavia, G., and Passmore, M. (2016b). *Influence of short rear end tapers on the wake of a simplified square-back vehicle: wake topology and rear drag*. *Experiments in Fluids*, 57(11):169

# Thank you!

[G.Pavia@lboro.ac.uk](mailto:G.Pavia@lboro.ac.uk)



Loughborough  
University